Kela, Petteri; Costa, Mário; Turkka, Jussi; Leppänen, Kari ; Jäntti, Riku

Flexible Backhauling with Massive MIMO for Ultra-Dense Networks

Published in:
IEEE Access

DOI:
10.1109/ACCESS.2016.2634039

Published: 27/01/2017

Document Version
Publisher's PDF, also known as Version of record

Published under the following license:
Other

Please cite the original version:
Kela, P., Costa, M., Turkka, J., Leppänen, K., & Jäntti, R. (2017). Flexible Backhauling with Massive MIMO for Ultra-Dense Networks. *IEEE Access*, *4*, 9625-9634. Article 7762799.
https://doi.org/10.1109/ACCESS.2016.2634039

Received October 28, 2016, accepted November 18, 2016, date of publication December 1, 2016, date of current version January 27, 2017.

Digital Object Identifier 10.1109/ACCESS.2016.2634039

Flexible Backhauling With Massive MIMO for Ultra-Dense Networks

PETTERI KELA[1,2], MÁRIO COSTA[1], JUSSI TURKKA[3], KARI LEPPÄNEN[1], AND RIKU JÄNTTI[2]
[1]Huawei Technologies Oy (Finland) Company, Ltd., 00180 Helsinki, Finland
[2]Department of Communications and Networking, Aalto University, 02150 Espoo, Finland
[3]European Communications Engineering Ltd., 02150 Espoo, Finland

Corresponding author: P. Kela (petteri.kela@huawei.com)

ABSTRACT One of the main challenges for wide-scale deployment and timely adoption of ultra-dense networks (UDNs) in future 5G is the backhaul. Typically, mmW technologies for backhaul require line-of-sight conditions while high-capacity wired-based solutions need a significant investment in infrastructure. Such limitations pose practical constrains on the scalability of UDNs and increase the deployment cost of dense networks. In this paper, we consider in-band backhaul for UDNs based on massive MIMO systems in sub-6 GHz. In particular, we propose a scheme for allowing simultaneous downlink transmissions in backhaul and access network on a single frequency band that exploits a novel combination of the state-of-the-art practical transmit and receive beamforming techniques. A novel frame structure for allowing a co-existence between massive MIMO-based backhaul and UDNs is also proposed. Moreover, a solution for in-band uplink transmissions that exploits time-division-duplex (TDD) and spatial multiple-access is also provided. Extensive numerical results using a realistic system-level simulator are given. Results show that the performance of a UDN with the proposed in-band backhaul scheme reaches ~58% of the throughput of a similar access network with ideal (e.g., wired) backhaul. Our results also show that the proposed scheme provides an increase in the throughput of ~30% compared with a TDD scheme for in-band backhaul. Further advantages of the proposed massive MIMO-based in-band backhaul scheme for UDNs include reusing both the (scarce) spectrum in sub-6 GHz and acquired macro-sites, thus providing a seamless transition from LTE to 5G networks.

INDEX TERMS Ultra-dense networks, massive MIMO, vehicular users, 5G.

I. INTRODUCTION

The exponential increase in demand for multimedia services and mobile broadband along with the requirements set by the fourth industrial revolution, including internet-of-things (IoT), industrial internet, massive machine-type communications (mMTC), vehicle-to-vehicle (V2V) and vehicle-to-infrastructure (V2I) communications, have confirmed the need for a new wireless communication standard, namely 5G. The targets set by operators and vendors for 5G typically include latencies below 1 ms, an area capacity of 1 Tbps/km^2, and support for a 100x increase in connected devices compared to that of Long Term Evolution-Advanced (LTE-A) [1]. Another common requirement for 5G is a minimum user-throughput of 50Mbps for everyone [2]. This includes vehicular users in urban environments. Therefore, 3rd generation partnership project (3GPP) has set a requirement that the next generation of radio access shall efficiently support users with velocities up to 30km/h in dense urban environments [3].

Network densification is commonly seen as a natural way of evolving towards 5G [4]. In particular, UDNs with a continuous coverage, i.e. continuous ultra-dense networks (C-UDNs), have been shown to be an attractive approach for achieving the aforementioned targets for 5G in sub-6 GHz, especially for vehicular and mobile users [5]. In fact, the performance of practical massive multiple-input multiple-output (M-MIMO) systems with macro- or micro-cell deployments is limited by channel aging and pilot contamination [5], [6]. Scenarios with stationary or quasi-static users allow for exploiting in a more efficient and practical manner the benefits of M-MIMO systems in terms of degrees-of-freedom, large array gain and subsequent low-transmit power, as well as low-cost of site acquisition and reuse.

Wide-scale deployment of C-UDNs requires backhaul solutions that are cost effective, reliable and scalable [7]. In particular, wired backhaul is typically seen as an infeasible approach for UDNs due to the high-cost of deployment [8]. On the other hand, millimeter wave (mmW) based solutions typically require line-of-sight (LoS) conditions between the aggregation point and the UDN-access nodes (ANs), or proper network planning [9]. However, thorough cell planning typically increases the deployment cost of the network and limits the scalability of such an approach. Moreover, the decision made at the 2015 world radio communication conference (WRC'15) of postponing regulatory aspects of mmW-bands for mobile broadband communications to 2019 [10], provide an incentive for backhaul solutions that operate in sub-6 GHz and possibly in-band with the access network. This is particularly relevant due to the limited available spectrum in sub-6 GHz, and allows for a timely adoption of 5G by the year 2020.

FIGURE 1. **Illustration of wireless backhaul for 5G ultra-dense networks deployed on lamp-posts.**

This paper considers a two-tier architecture where the access network is based on a C-UDN, and an M-MIMO system provides wireless backhaul between the UDN-ANs and the aggregation points (or M-MIMO-ANs). This is illustrated in Fig. 1. We focus on a sub-6 GHz solution for in-band backhaul of dense networks. In particular, we propose a scheme for allowing simultaneous in-band downlink (DL) transmissions in backhaul and access network that exploits a novel combination of state-of-the-art practical transmit and receive beamforming techniques. A novel frame structure for in-band operation of UDN and M-MIMO based backhaul is also proposed. In uplink (UL), a time division duplex (TDD) mode of operation is employed in order to share the radio resources between the backhaul and access network. We provide extensive numerical results using a realistic system-level simulator thus allowing one to assess the expected achievable throughput of an in-band backhaul solution operating at sub-6 GHz in future 5G networks.

This paper is related to the work in [11] and [12] where in-band M-MIMO solutions for wireless backhaul of UDNs in sub-6 GHz are also considered. In particular, the analysis in [11] assumes that each UDN-AN is associated with a single user node (UN) on a given time-frequency resource, i.e. multi-user multiple-input multiple-output (MIMO) (MU-MIMO) in the access network is not considered. Moreover, the interference caused to the UN from neighboring UDN-ANs is assumed negligible. Finally, an uncorrelated Rayleigh fading channel model is used in [11] and perfect channel state information (CSI) at transmitter (CSIT) is assumed therein. The work in [12] focuses on the case where the UDN-ANs may have full-duplex capabilities. However, single-antenna UDN-ANs are assumed, and independent and identically distributed (iid) channels are considered, i.e. spatial correlation is not taken into account. Our work considers multiantenna transceivers at the ANs and the numerical results provided in this paper are based on a realistic ray-tracing channel model.

This paper is also related to the work in [9] where MU-MIMO techniques are proposed for providing high-capacity links to small cells. However, the work in [9] considers mmW frequencies for the backhaul and assumes that the access network operates at different frequencies than that of the backhaul. Our paper considers in-band simultaneous DL transmissions in the backhaul and access network, and proposes modifications to state-of-the-art MU-MIMO techniques in order to mitigate in-band interference. Our work considers a sub-6 GHz operating frequency and provides extensive numerical results that allow one to assess the performance of a practical in-band backhaul scheme in terms of system throughput. Note that the path-loss at sub-6 GHz is significantly smaller than that in mmW frequencies, and the interference caused by in-band backhaul to the access network is typically higher for sub-6 GHz systems. Hence, state-of-the-art MU-MIMO techniques need to be modified in order to mitigate in-band interference. This is considered herein.

In particular, multiple UNs are scheduled simultaneously on the same time-frequency resources, and these UNs are equipped with multiantenna transceivers. Transmit (in UL) and receive (in DL) beamforming are employed by the UNs, and each user is associated with a single spatial data-stream. The association between UN and AN is dynamic and may change within a few transmission time intervals (TTIs) depending on the channel quality. A given UN is scheduled by a single AN, and Coordinated Multi-Point (CoMP) transmissions are not considered. Hence, the network synchronization requirements of our approach are not as stringent as in CoMP. Also, CoMP schemes are typically sensitive to channel aging, and in this paper emphasis is given to mobile UNs that can have velocities of around 50 km/h. Nevertheless, a mild coordination among UDN-ANs is still needed in our scheme for sharing scheduling decisions and interference information for link adaptation purposes. Otherwise, we consider that the ANs are independent and have individual baseband processing. This differentiates our solution from a typical cloud radio access network.

In the MU-MIMO type of solution considered herein for the backhaul, multiple spatial streams are allowed on each backhaul link between a M-MIMO-AN and a UDN-AN. Each UDN-AN consists of two antenna arrays in order to allow for simultaneous in-band DL transmissions in the backhaul and access network. This is illustrated in Fig. 1 where such a UDN-AN is deployed on a lamppost. The "self-interference" of such UDN-AN is taken into account herein and a simple scheme for interference cancellation is proposed. We note that a full-duplex solution would avoid the need of having two antenna arrays on each UDN-ANs [11]–[13]. However, it is likely that the first release of 5G, expected to be deployed by the year 2020, will mainly make use of TDD and frequency division duplex (FDD) operation modes. Hence, full-duplex is not considered in this paper. The interested reader is referred to [11]–[13] and references therein.

The remainder of this paper is organized as follows. Section II provides the systems models employed in this paper. In Section III, a novel frame structure is proposed for in-band operation of wireless backhaul and access network. Section IV describes how state-of-the-art MU-MIMO schemes can be modified in order to mitigate co-channel interference due to in-band simultaneous transmission in backhaul and access network. Focus is given to vehicular users and dense networks. Section V describes a simple TDD based scheme for UL transmissions in the backhaul and UDN. Section VI provides extensive numerical results using a realistic system-level simulator. Finally, Section VII concludes the paper.

II. SYSTEM MODEL

This section provides the system models used throughout the paper. In particular, the expression for the backhaul signal received at the jth ($j \in \{1, \ldots, J\}$) UDN-AN and transmitted by the lth ($l \in \{1, \ldots, L\}$) M-MIMO-AN on the kth ($k \in \{1, \ldots, K\}$) spatial stream is[1]

$$y^B_{j,l,k} = z^{B^H}_{j,k} \boldsymbol{H}^B_{j,l} \boldsymbol{w}^B_{j,l,k} x^B_{j,l,k} + i^B_{j,l,k} + \eta_j, \tag{1}$$

where $\boldsymbol{H}^B_{j,l} \in \mathbb{C}^{M^B_{\text{Rx}} \times M^B_{\text{Tx}}}$ denotes the MIMO channel matrix between the lth M-MIMO-AN and the jth UDN-AN, and $(\cdot)^H$ denotes conjugate transpose. Moreover, vector $\boldsymbol{w}^B_{j,l,k} \in \mathbb{C}^{M^B_{\text{Tx}}}$ denotes the precoder for the kth spatial stream, employed by the lth transmitting M-MIMO-AN to the jth receiving UDN-AN while $z^B_{j,k} \in \mathbb{C}^{M^B_{\text{Rx}}}$ denotes the receive beamforming vector for the kth spatial stream and jth UDN-AN. In addition, $x^B_{j,l,k} \in \mathbb{C}$ in (1) denotes the (backhaul) symbol transmitted at the kth spatial stream by the lth M-MIMO-AN to the jth receiving UDN-AN. Finally, $i^B_{j,l,k} \in \mathbb{C}$ and $\eta_j \in \mathbb{C}$ denote the interference experienced at the jth UDN-AN for the signal transmitted by the lth M-MIMO-AN on the kth spatial stream, and measurement noise, respectively. In particular, measurement noise is modeled as zero-mean complex-circular Gaussian with variance σ^2_j. Also, $i^B_{j,l,k}$ takes into account interference due to other M-MIMO-ANs and spatial streams, except the kth spatial stream associated with the lth AN, as well as the self-interference that takes place from co-locating the backhaul UDN-AN receiver and the access-network UDN-AN transmitter. More precisely, $i^B_{j,l,k}$ is given by

$$\begin{aligned} i^B_{j,l,k} = &\sum_{\ell=1}^{L} \sum_{\substack{\kappa=1 \\ \kappa \neq k_l}}^{K} z^{B^H}_{j,k} \boldsymbol{H}^B_{j,\ell} \boldsymbol{w}^B_{j,\ell,\kappa} x^B_{j,\ell,\kappa} \\ &+ \sum_{\iota=1}^{J} \sum_{n=1}^{N} z^{B^H}_{j,k} \tilde{\boldsymbol{H}}^B_{j,\iota} \boldsymbol{w}^A_{\iota,n} x^A_{\iota,n}. \end{aligned} \tag{2}$$

Here, $\tilde{\boldsymbol{H}}^B_{j,l} \in \mathbb{C}^{M^B_{\text{Rx}} \times M^A_{\text{Tx}}}$ denotes the self-interference MIMO channel. Moreover, vector $\boldsymbol{w}^A_{\iota,n} \in \mathbb{C}^{M^A_{\text{Tx}}}$ denotes the (access-network) precoder employed by the ιth UDN-AN to the nth UN and $x^A_{\iota,n} \in \mathbb{C}$ denotes the corresponding transmitted symbol. The number of UDN-ANs and UNs are denoted by J and N, respectively.

For the access-network, the signal received at the nth UN and transmitted by the jth UDN-AN is

$$y^A_{n,j} = z^{A^H}_{n} \boldsymbol{H}^A_{n,j} \boldsymbol{w}^A_{n,j} x^A_{n,j} + i^A_n + \eta_n, \tag{3}$$

where $\boldsymbol{w}^A_{n,j} \in \mathbb{C}^{M^A_{\text{Tx}}}$ and $z^A_n \in \mathbb{C}^{M^A_{\text{Rx}}}$ denote the precoder employed at the jth UDN-AN to the nth UN and the corresponding receive beamforming weight vector employed by the nth UN, respectively. Moreover, $x^A_{n,j} \in \mathbb{C}$ denotes the symbol intended to the nth UN and transmitted by the jth UDN-AN. In (3), $i^A_{n,j} \in \mathbb{C}$ denotes the interference observed by the nth UN when served by the jth UDN-AN and $\eta_n \in \mathbb{C}$ denotes zero-mean complex-circular Gaussian measurement noise at the nth UN. In particular, the interference that the nth UN observes includes that due to backhaul transmissions as well as interference from other UDN-ANs, i.e.:

$$i^A_n = \sum_{\substack{\eta=1 \\ \eta \neq n}}^{N} \sum_{\iota=1}^{J} z^{A^H}_n \boldsymbol{H}^A_{n,\iota} \boldsymbol{w}^A_{\eta,\iota} x^A_{\eta,\iota} + \sum_{l=1}^{L} \sum_{k=1}^{K} z^{A^H}_n \tilde{\boldsymbol{H}}^A_{n,l} \boldsymbol{w}^B_{k,l} x^B_{k,l}, \tag{4}$$

where $\tilde{\boldsymbol{H}}^A_{n,l} \in \mathbb{C}^{M^A_{\text{Rx}} \times M^B_{\text{Tx}}}$ denotes the MIMO (interfering) channel between the lth M-MIMO-AN and the nth UN.

In UL, the backhaul signal received at the lth M-MIMO-AN, on the kth spatial stream, and transmitted by the jth UDN-AN is

$$\tilde{y}^B_{j,l,k} = \tilde{z}^{B^H}_{j,l,k} \boldsymbol{H}^{B^T}_{j,l} \tilde{\boldsymbol{w}}^B_{j,k} \tilde{x}^B_{j,k} + \tilde{i}^B_{j,l,k} + \eta_l, \tag{5}$$

where $\tilde{z}^B_{j,l,k} \in \mathbb{C}^{\tilde{M}^B_{\text{Rx}}}$ denotes the receive beamforming vector employed at the lth M-MIMO-AN for the kth spatial stream from the jth UDN-AN while $\tilde{\boldsymbol{w}}^B_{j,k} \in \mathbb{C}^{\tilde{M}^B_{\text{Tx}}}$ represents the precoder employed by the jth UDN-AN for the kth spatial stream. Also, $\tilde{x}^B_{j,k} \in \mathbb{C}$ denotes the UL backhaul signal transmitted by the jth UDN-AN on the kth spatial stream. Moreover, $\tilde{i}^B_{j,l,k} \in \mathbb{C}$ denotes the interference observed at

[1]For the sake of clarify we consider the case when all UDN-ANs receive equal amount of spatial streams. Moreover, we focus on the case where each UDN-AN is served by a single M-MIMO-AN. The extension is straightforward.

the lth M-MIMO-AN for the kth stream transmitted by the jth UDN-AN, and it is given by

$$\tilde{i}^B_{j,l,k} = \sum_{\iota=1}^{J}\sum_{\substack{\kappa=1\\ \kappa\neq k_l}}^{K} \tilde{z}^{B^H}_{j,l,k} \boldsymbol{H}^{B^T}_{j,\iota}\tilde{\boldsymbol{w}}^B_{\iota,\kappa}\tilde{x}^B_{\iota,\kappa}. \tag{6}$$

Finally, the signal received in UL at the jth UDN-AN and transmitted by the nth UN is

$$\tilde{y}^A_{j,n} = \tilde{z}^{A^H}_{j,n}\boldsymbol{H}^{A^T}_{n,j}\tilde{\boldsymbol{w}}^A_n\tilde{x}^A_n + \tilde{i}^A_{j,n} + \eta_j, \tag{7}$$

where $\tilde{z}^A_{j,n} \in \mathbb{C}^{\tilde{M}^A_{\mathrm{Rx}}}$ denotes the receive beamforming vector employed by the jth UDN-AN for the nth UN. Moreover, vector $\tilde{\boldsymbol{w}}^A_n \in \mathbb{C}^{\tilde{M}^A_{\mathrm{Tx}}}$ denotes the precoder employed by the nth UN and $\tilde{x}^A_n \in \mathbb{C}$ denotes the corresponding transmitted symbol. In (7), $\tilde{i}^A_{j,n} \in \mathbb{C}$ models the multiple access interference and η_j denotes measurement noise at the jth UDN-AN. In particular, the multiple access interference is given by

$$\tilde{i}^A_{j,n} = \sum_{\substack{\eta=1\\ \eta\neq n}}^{N} \tilde{z}^{A^H}_{j,n}\boldsymbol{H}^{A^T}_{\eta,j}\tilde{\boldsymbol{w}}^A_\eta\tilde{x}^A_\eta. \tag{8}$$

In sections IV and V, the transmit and receive beamforming weight vectors employed in both backhaul and access network are given.

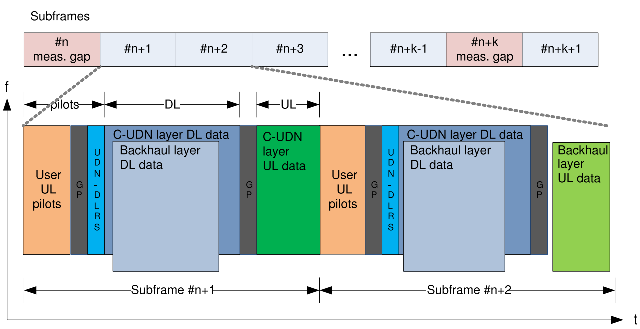

FIGURE 2. Proposed TDD frame structure for in-band inter-operation of M-MIMO based backhaul and UDN. Simultaneous in-band DL transmissions for backhaul and UDN are allowed while the corresponding UL transmissions are separated in the time domain.

III. PROPOSED FRAME STRUCTURE

A novel radio frame structure is proposed in this section for supporting in-band backhaul of UDNs using macro cell M-MIMO base stations. Figure 2 illustrates the proposed frame structure as well as backhaul measurement gaps with a periodicity of k subframes. Our frame structure can be understood as comprising the same building blocks as typical frame structures for cellular communication systems. However, the actual frame structure illustrated in Fig. 2 is novel. In particular, DL data transmissions on the access network and backhaul occur simultaneously by exploiting spatial division multiplexing (SDM) schemes. Time synchronization between both layers is required in order to ensure interference-free UL data transmissions. Each subframe consists of UL reference signals sent by the UNs as well as DL and UL data transmissions [5]. Moreover, DL data transmissions start with precoded DL reference signals that are exploited by UNs in order to design receive beamforming weight vectors [14]. Guard periods (GPs) are also placed at every switching point of the communication link direction in order to accommodate for hardware delays.

The UL reference signals (also called pilots or beacons) transmitted periodically by the UNs are measured by one or more UDN-ANs and make it possible to support a truly user-centric mobility scheme, thus representing a paradigm shift from legacy cellular networks to borderless C-UDNs [5]. Periodic CSI reporting and handovers triggered by the UN are thus not required. Hence, the proposed frame structure employs a TDD operation mode that allows exploiting channel reciprocity and dynamic traffic allocation when compared to FDD. The proposed frame structure provides enough resources for UL reference signals thus allowing the network to track the positions of the UNs [15] and maintain up-to-date CSIT with low pilot contamination from all active users [5]. Note also that backhaul transmissions are muted during transmission of UL reference signals. Such a requirement avoids uncontrolled pilot contamination which typically impair the performance of MU-MIMO systems significantly.[2]

The frame structure illustrated in Fig. 2 separates the UL data transmissions occurring in the access network and backhaul by means of TDD. This is because UL transmissions from the UNs interfere significantly with the backhaul UL signals even when the UNs are equipped with multiantenna transceivers and employ UL precoding. In fact, we have observed that the electrical-size of multiantenna transceivers typically employed by UNs is not sufficiently large to allow highly-directive UL transmissions. Hence, the UL of backhaul and access network are separated flexibly in the time domain.

In the backhaul, a TDD mode of operation is also considered between UL and DL. This is useful for acquiring the CSIT and employing MU-MIMO schemes in M-MIMO systems in a practical manner by exploiting channel reciprocity. In particular, each backhaul multiantenna transceiver that is deployed on the UDN-ANs transmit UL reference signals from all of its antennas in orthogonal radio resources.[3] Measurement gaps in the access network are used in order to mute the UNs and avoid interference to the backhaul. For example, if the measurement gaps occur once every 5 ms, then only a 4 % overhead is caused by backhaul pilots, given that a 0.2 ms subframe length is assumed as proposed in [5]. Thus, in order to make such measurement gap configuration sufficient and enable multi-stream backhaul transmissions with access link interference cancellation, antenna arrays

[2] Simultaneous transmission of UL reference signals are still allowed and taken into account in Section VI.

[3] In the backhaul, transmissions from the UDN-ANs to the M-MIMO-ANs are termed UL. Recall also that each UDN-AN employs two multiantenna tranceivers: one for the backhaul and another for the access link.

with few antennas can be utilized in backhaul receiver arrays. Moreover, the M-MIMO base station can utilize a fraction of the measurement gap, e.g. one symbol, for transmitting downlink reference signals (DLRSs) [16]. Such precoded DLRSs can be used by the C-UDN-ANs in order to calculate receive beamforming weight vectors, thus enhancing the desired backhaul transmissions. These precoded DLRSs can also be exploited by the UNs for mitigating the in-band interference from DL backhaul transmissions.

TABLE 1. Example of 5G numerologies for in-band backhaul of C-UDN based on M-MIMO.

parameter	C-UDN	M-MIMO
Bandwidth [MHz]	200	200
Subcarrier spacing [kHz]	240	60
Symbol length [us]	4.1667	16.6667
Subcarriers FFT size	1024	4096
Effective subcarriers	833	3333
TTI duration [ms]	0.2	0.2
Number of GPs	2	-
Symbols per subframe	42	8
CP duration [us]	0.57	4.7
GP duration [us]	0.53	-

Table 1 provides numerologies for C-UDN and M-MIMO layers. In particular, TTI lengths are aligned in order to enable flexible TDD and SDM operation. In this proposal, the symbol length for C-UDN is different from that of the M-MIMO system, but still both DL and UL can be embedded within one subframe; see Fig. 2. For example, if 28 C-UDN orthogonal frequency division multiplexing (OFDM) symbols are allocated to form a DL time slot and 10 symbols for the corresponding UL time slot, then 6 OFDM symbols can be allocated for DL backhaul and 2 symbols can assigned for UL backhaul. The benefit of such a configuration is that for reasonably-sized macro cells, timing advance can be tackled during the same UL/DL slots including GPs. Note that it is possible to utilize exactly the same numerologies for both backhaul and UDN layers, but then the UL reference signals intended to handle user mobility and channel estimation will increase the overhead.

IV. DOWNLINK PRECODER AND RECEIVE FILTER DESIGN

Precoder and receive filter designs have an important role in dealing with interference when two co-located wireless networks share the same time-frequency resources. This section provides details of the employed state-of-the-art MU-MIMO schemes, and needed modifications for in-band interference mitigation, that allow for in-band simultaneous DL transmissions in the backhaul and access network.

In DL backhaul, a major challenge is to design receive filters for the UDN-ANs in a manner that the self-interference due to DL transmissions in the access network is mitigated.[4] In backhaul, channel aging is not severe since the UDN-ANs are typically stationary. Moreover, the UDN-ANs are geographically distributed with an inter-site distance (ISD) of tens of meters, thus making it possible to exploit the large degrees-of-freedom provided by the M-MIMO system for employing MU-MIMO schemes. In the UDN layer, the major challenge is to design precoders and receive filters so that mobile users can receive DL transmissions efficiently and without significant interference from DL backhaul transmissions.

[4]Here, self-interference refers to the interference caused by two multi-antenna transceivers co-located at each UDN-AN.

A. PRECODER AND RECEIVE FILTER DESIGN FOR BACKHAUL TRANSMISSIONS

We employ the block diagonalization (BD) algorithm [17] for designing the precoders employed by the M-MIMO-AN as well as the receive beamformers used by the backhaul UDN-ANs. Here, we give a brief review of the BD algorithm, which may be understood as an extension of the zero-forcing (ZF) precoder to cases where the receivers are equipped with multiantenna transceivers. In particular, the BD algorithm requires acquiring the MIMO CSI at the M-MIMO-AN from all UDN-ANs and signalling the receive beamformers on a DL control channel. Alternatively, the M-MIMO-AN can design the precoders either by taking into account a single antenna at the UDN-ANs or by assuming that a certain receive beamformers are used by the UDN-ANs. In such a case, the M-MIMO-AN transmits precoded DL reference signals that allow the UDN-ANs to design the receive beamformers. Herein, we consider the approach where the M-MIMO-AN designs both transmit and receive beamformers since the goal is to increase the throughput of the backhaul channel. It should be noted that the approach taken in this paper leads to an increase in overhead due to CSIT and DL signalling. However, in practice such an overhead is not overwhelming due to the typically small number of antennas at each backhaul UDN-AN and the large channel coherence time since both transmitter and receivers are stationary.

The BD algorithm has several advantages when compared to other schemes. Even though it is suboptimal it is a non-iterative scheme and provides a good trade-off between complexity and performance. For example, the matched filter (MF) precoder is typically used in M-MIMO systems when complexity is the main limiting factor. However, the performance of MF in practical M-MIMO systems is rather limited due to high inter-beam interference [5]. On the other hand, ZF precoder typically leads to a prohibitively high transmit power since it aims at transmitting as many spatial streams as the total number of receiving antennas [17].

The transmit and receive beamforming vectors obtained with the BD algorithm are found as follows. Let $\boldsymbol{U}_{j,l} \in \mathbb{C}^{M^B_{\mathrm{Rx}} \times M_s}$ denote the left singular vectors of $\boldsymbol{H}^B_{j,l}$ corresponding to the $M_s \in \mathbb{N}$ largest singular values. M_s denotes the number of spatial streams for each backhaul UDN-AN, and it is a design parameter that depends on channel conditions, scheduler, among other factors. Here, we assume that M_s is identical for all UDN-ANs. Let $\bar{\boldsymbol{H}}^B_{j,l} = \boldsymbol{U}^H_{j,l}\boldsymbol{H}^B_{j,l}$ and define $\bar{\boldsymbol{H}}^B_l \in \mathbb{C}^{M_s J \times M^B_{\text{Tx}}}$ as well as $\tilde{\boldsymbol{H}}^B_{j,l} \in \mathbb{C}^{M_s(J-1)\times M^B_{\text{Tx}}}$ as follows

$$\bar{\boldsymbol{H}}^B_l = [\bar{\boldsymbol{H}}^{B^T}_{1,l} \ldots \bar{\boldsymbol{H}}^{B^T}_{J,l}]^T \tag{9}$$

$$\tilde{\boldsymbol{H}}^B_{j,l} = [\bar{\boldsymbol{H}}^{B^T}_{1,l}, \ldots, \bar{\boldsymbol{H}}^{B^T}_{j-1,l}, \bar{\boldsymbol{H}}^{B^T}_{j+1,l}, \bar{\boldsymbol{H}}^{B^T}_{J,l}]^T. \tag{10}$$

The precoders are found by first finding the right singular-vectors, denoted by $\tilde{\boldsymbol{V}}_j \in \mathbb{C}^{M^B_{\text{Tx}}\times(M^B_{\text{Tx}}-(M_s(J-1)))}$, corresponding to the $(M^B_{\text{Tx}} - (M_s(J-1)))$ smallest singular-values of $\tilde{\boldsymbol{H}}^B_{j,l}$ and subsequently determining the right singular-vectors, denoted by denoted by $\boldsymbol{V}_j \in \mathbb{C}^{M^B_{\text{Tx}}\times M_s}$, corresponding to the M_s largest singular-values of $\bar{\boldsymbol{H}}^B_{j,l}\tilde{\boldsymbol{V}}_j$. The precoder matrix $\boldsymbol{W}^B_{j,l} \in \mathbb{C}^{M^B_{\text{Tx}}\times M_s}$ for the lth M-MIMO-AN towards the jth UDN-AN is then given by

$$\boldsymbol{W}^B_{j,l} = \tilde{\boldsymbol{V}}_j\boldsymbol{V}_j, \tag{11}$$

where we have considered an equal power-allocation scheme. The corresponding receive beamforming matrix for the jth UDN-AN $\boldsymbol{Z}^B_j \in \mathbb{C}^{M^B_{\text{Rx}}\times M_s}$ is given by

$$\boldsymbol{Z}^B_j = \boldsymbol{U}_{j,l}\tilde{\boldsymbol{U}}_j, \tag{12}$$

where $\tilde{\boldsymbol{U}}_j \in \mathbb{C}^{M_s\times M_s}$ denotes the left singular vectors of $\bar{\boldsymbol{H}}^B_{j,l}\tilde{\boldsymbol{V}}_j$.

The DL signal-to-interference-plus-noise ratio (SINR) experienced by the jth ($j \in \{1,\ldots,J\}$) UDN-AN being served by the lth ($l \in \{1,\ldots,L\}$) M-MIMO-AN and for the kth ($k \in \{1,\ldots,K\}$) spatial stream is:

$$\text{SINR}^{DL}_{j,l,k} = \frac{P_{j,l,k}|\boldsymbol{z}^{B^H}_{j,k}\boldsymbol{H}^B_{j,l}\boldsymbol{w}^B_{j,l,k}|^2}{\sum\limits_{\ell=1}^{L}\sum\limits_{\substack{\kappa=1\\ \kappa\neq k_l}}^{K} P_{\ell,\kappa}|\boldsymbol{z}^{B^H}_{j,k}\boldsymbol{H}^B_{j,\ell}\boldsymbol{w}^B_{\ell,\kappa}|^2 + I^B_{j,k} + \sigma^2_j}, \tag{13}$$

$$I^B_{j,k} = \sum_{\iota=1}^{J}\sum_{n=1}^{N} P_{\iota,n}|\boldsymbol{z}^{B^H}_{j,k}\tilde{\boldsymbol{H}}^B_{j,\iota}\boldsymbol{w}^A_{\iota,n}|^2, \tag{14}$$

where $P_{j,l,k} \in \mathbb{R}$ denotes the transmit power allocated to the kth spatial stream at the lth M-MIMO-AN for the jth UDN-AN and $P_{\iota,n} \in \mathbb{R}$ denotes power allocated to the n UN at the ith UDN-AN.

B. PRECODER AND RECEIVE FILTER DESIGN FOR UDN ACCESS

We employ MF precoding at the UDN-ANs for DL transmissions in the access network in a multi-user multiple-input single-output (MU-MISO) fashion. In particular, each UN is assigned a single spatial stream even though UNs may have multiantenna receivers. This is done in order to reduce the UL pilot signalling overhead and avoid estimating the channel from multiple antennas. Multiantenna receivers are exploited for receive beamforming including also possibility for mitigating backhaul interference. Moreover, each UN is served by a single UDN-AN, and CoMP transmissions are not considered herein. MF precoding is used since it is more robust than ZF to channel aging and more efficient than BD in terms of control signalling overhead [5]. This is particularly important for providing 5G services in urban environments to mobile users with velocities ranging from 30km/h to 50km/h. Moreover, the UL reference signals sent by the UNs for CSIT and design of MF precoders are transmitted from a single antenna-element of the multiantenna UNs. This is done in order to reduce the control signalling overhead.

Let $\boldsymbol{h}_{n,j} \in \mathbb{C}^{M^A_{\text{Tx}}}$ denote the DL multiple-input-single-output (MISO) channel between the jth multiantenna UDN-AN and the nth UN. Recall that the UNs may have multiantenna transceivers, but for the sake of reducing the control signalling overhead, the channel from only one antenna-element of the UN is estimated. In particular, $\boldsymbol{h}_{n,j}$ is estimated from UL reference signals by exploiting the channel reciprocity and a TDD mode of operation between UL and DL. Let $\boldsymbol{H}^A_j \in \mathbb{C}^{M^A_{\text{Tx}}\times N}$ denote the corresponding MISO channels for $N \in \mathbb{N}$ scheduled UNs. The DL precoder matrix at the jth UDN-AN for the N scheduled UNs is simply given by $\boldsymbol{W}^A_j = \boldsymbol{H}^{A^H}_j$.

The receive beamforming vectors for the access-network are designed at the UNs by means for precoded DL reference signals transmitted by the UDN-ANs [16]. Note that this is different from the approach taken in the backhaul where the M-MIMO-ANs designed both transmit and receive beamforming vectors. Such a decentralized approach is taken in here for the access-network in order to reduce control signalling overhead, which is particularly important in cases of high user density and mobility scenarios with short coherence times. Moreover, designing the receive beamforming vectors for the UNs requires taking into account the DL interference from the backhaul. Hence, the UNs also exploit the DL reference signals transmitted from the M-MIMO-ANs in designing the receive beamforming vectors. In particular, the DL channel matrix observed by the nth UN scheduled by the jth UDN-AN is given by

$$\bar{\boldsymbol{H}}^A_n = \left[\sum\nolimits_{j=1}^{J}\boldsymbol{H}^A_{n,j}\sum\nolimits_{i=1}^{N}\boldsymbol{w}^A_{i,j}\ \sum\nolimits_{l=1}^{L}\tilde{\boldsymbol{H}}^A_{n,l}\sum\nolimits_{k=1}^{K}\boldsymbol{w}^B_{l,k}\right]. \tag{15}$$

The receive beamforming vector $\boldsymbol{z}^A_n \in \mathbb{C}^{M^A_{\text{Rx}}}$ for the nth UN corresponds to the first row of the Moore-Penrose pseudo-inverse of $\bar{\boldsymbol{H}}^A_n$. Note that all precoded DL reference signals are transmitted simultaneously in order to reduce the overhead for channel estimation.

The DL SINR experienced by the nth UN being served by the jth UDN-AN is

$$\text{SINR}^{DL}_{n,j} = \frac{P_{n,j}|\boldsymbol{z}^{A^H}_n\boldsymbol{H}^A_{n,j}\boldsymbol{w}^A_{n,j}|^2}{\sum\limits_{\substack{\eta=1\\ \eta\neq n}}^{N}\sum\limits_{\iota=1}^{J} P_{\eta,\iota}|\boldsymbol{z}^{A^H}_n\boldsymbol{H}^A_{n,\iota}\boldsymbol{w}^A_{\eta,\iota}|^2 + I^A_n + \sigma^2_n}, \tag{16}$$

where $P_{n,j}$ denotes the transmit power allocated to precoder $\boldsymbol{w}^A_{n,j}$. Moreover, $I^A_n \in \mathbb{R}$ denotes the interference experienced by the nth UN that is caused by DL backhaul transmissions, and it is given by

$$I_n^A = \sum_{l=1}^{L} \sum_{k=1}^{K} P_{k,l} |\boldsymbol{z}_n^{A^H} \tilde{\boldsymbol{H}}_{n,l}^A \boldsymbol{w}_{k,l}^B|^2. \tag{17}$$

V. UPLINK PRECODER AND RECEIVE FILTER DESIGN

The employed precoder and receive filter design for backhaul transmissions in UL consist in reusing the beamforming vectors from DL in UL. In particular, the precoder employed by the jth UDN-AN for the kth spatial stream is $\tilde{\boldsymbol{w}}_{j,k}^B \triangleq \boldsymbol{z}_{j,k}^B$. Similarly, the receive beamforming vector employed by the lth M-MIMO-AN for the kth spatial stream and transmitted by the jth UDN-AN is $\tilde{\boldsymbol{z}}_{j,l,k}^B \triangleq \boldsymbol{w}_{j,l,k}^B$. The corresponding SINR experienced at the lth M-MIMO-AN for the kth spatial stream transmitted by the jth UDN-AN is

$$\mathrm{SINR}_{j,l,k}^{UL} = \frac{P_{j,k} |\tilde{\boldsymbol{z}}_{j,l,k}^{B^H} \boldsymbol{H}_{j,l}^{B^T} \tilde{\boldsymbol{w}}_{j,k}^B|^2}{\sum\limits_{\iota=1}^{J} \sum\limits_{\substack{\kappa=1 \\ \kappa \neq k_\iota}}^{K} P_{\iota,\kappa} |\tilde{\boldsymbol{z}}_{j,l,k}^{B^H} \boldsymbol{H}_{j,\iota}^{B^T} \tilde{\boldsymbol{w}}_{\iota,\kappa}^B|^2 + \sigma_l^2}. \tag{18}$$

In the access network, the precoder employed by the nth UN is a MF that is found from the precoded DL reference signals as follows

$$\tilde{\boldsymbol{w}}_n^A = \left(\sum_{j=1}^{J} \boldsymbol{H}_{n,j}^A \sum_{i=1}^{N} \boldsymbol{w}_{i,j}^A \right)^H. \tag{19}$$

Note that the precoded DL reference signals are transmitted simultaneously by all UDN-ANs for all scheduled UNs. This is done in order to reduce the overhead due to channel estimation. However, the leakage inherent of such an approach is not significant due to the employed electrically-large antenna arrays at the UDN-ANs and LoS conditions in UDNs. Extensive numerical results presented in Section VI confirm this observation. The receive beamforming vectors at the UDN-ANs are identical to those used for DL transmission. In particular, the receive beamforming vector employed by the jth UDN-ANs for the ith UN is $\tilde{\boldsymbol{z}}_{i,j}^A \triangleq \boldsymbol{w}_{i,j}^A$. The SINR experienced by the jth UDN-ANs for the nth UN is

$$\mathrm{SINR}_{n,j}^{UL} = \frac{P_n |\tilde{\boldsymbol{z}}_{i,j}^{A^H} \boldsymbol{H}_{n,j}^{A^T} \tilde{\boldsymbol{w}}_n^A|^2}{\sum\limits_{\substack{\eta=1 \\ \eta \neq n}}^{N} P_\eta |\tilde{\boldsymbol{z}}_n^{A^H} \boldsymbol{H}_{\eta,j}^{A^T} \tilde{\boldsymbol{w}}_\eta^A|^2 + \sigma_j^2}. \tag{20}$$

VI. EVALUATION OF THE PROPOSED IN-BAND BACKHAULING SOLUTION

This section illustrates the performance of the proposed solution for in-band backhaul of UDNs based on a M-MIMO system. In particular, the performance was assessed on our dynamic 5G system-level simulator; see also [5]. We have considered the Madrid grid as the deployment scenario for this numerical study [18]. The Madrid grid is illustrated in Fig. 3.

In order to follow 3GPP guidelines for next generation studies [3], we have considered a single unpaired 200 MHz bandwidth around a carrier frequency of 3.5 GHz. Three non-cooperative M-MIMO-ANs were deployed in order to serve as backhaul for 43 UDN-ANs. This is illustrated in Fig. 3. All three M-MIMO-ANs consisted of planar antenna arrays composed of 15 × 15 dual-polarized 3GPP patch antennas [19]. The planar arrays were placed and tilted

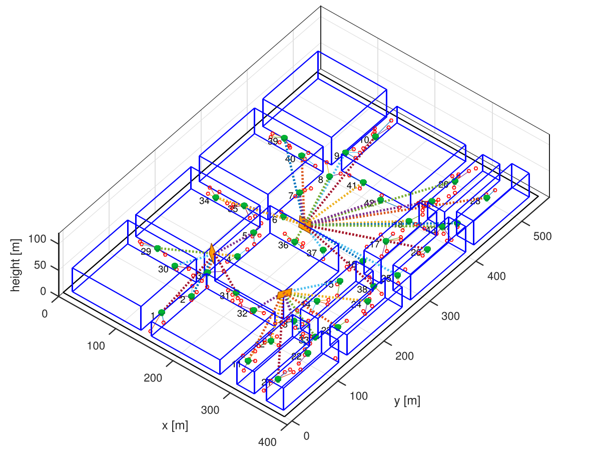

FIGURE 3. Deployment scenario for assessing the performance of the proposed solution for in-band backhaul of UDNs using M-MIMO systems. In particular, 43 UDN-ANs, illustrated as green dots, are placed in the edges of pavements of ordinary streets. On the pedestrian street and highway of the Madrid grid the UDN-ANs are placed at the center (equal distance from buildings). For the M-MIMO-ANs, planar arrays, illustrated as orange rectangles, are placed on the upper-edge of the walls of the center-most building and tilted towards street level.

TABLE 2. Parameters used for the numerical study.

Parameter	Value	
Simulation scenario	METIS Madrid Grid [22]	
Carrier bandwidth	Unpaired 200 MHz	
Center frequency	3.5 GHz	
Modulation scheme	OFDM	
Channel model	METIS map-based model [18]	
CSI beacon scheduling	Beacons: round robin in CSI age order with 25m CP compensation distance 250m beacon reuse distance [21]	
Data scheduling	Data: MT w/ rate CSI age weighting [21]	
Link Adaptation	Inner and outer loop	
Traffic model	Infinite buffer	
User nodes	1000 per km^2	
User node velocity	0 km/h and 50 km/h	
	C-UDN access layer	M-MIMO backhaul
Network (synchronous)	43 access nodes 20 TX ant./AN 5m antenna height	3 base stations 20x20 planar array/AN 52m antenna height
DL TX power budget	0, 10, 20 and 30 dBm per AN	49 dBm per base station
UL TX power	23 dBm per user	33 dBm per C-UDN AN
RX array model	2 RX antennas at user nodes with cross-dipoles	2 RX antennas at C-UDN access nodes with cross-dipoles 6m antenna height
TX array model	Circular array with 3GPP dual-polarized patch antennas [19]	Rectangular array with 3GPP dual-polarized patch antennas [19]
Array mechanical downtilt	0 degrees	7, 18 and 18 degrees [20]
CSI	Estimated from UL wideband beacons using LSE	Estimated from UL wideband C-UDN pilots using LSE

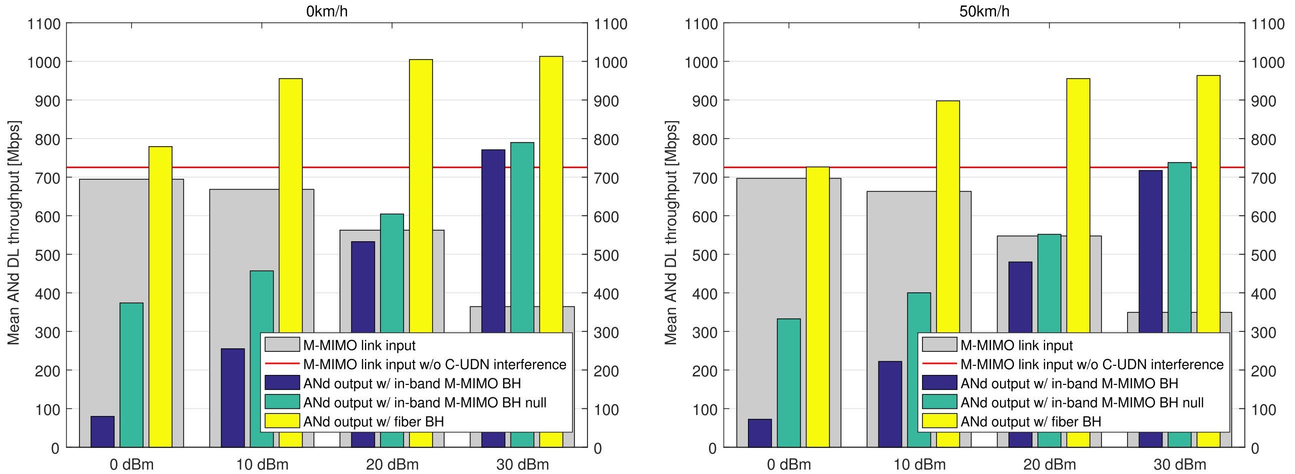

FIGURE 4. Performance of proposed solution for in-band backhaul of UDNs using a M-MIMO system in terms of DL throughput per UDN-AN. The green bars correspond to the case where users exploit the precoded DL reference signals transmitted by M-MIMO-ANs for mitigating backhaul interference. Results with ideal backhaul (e.g., wired connection) are also illustrated for comparison. Two different mobility scenarios are shown where users are either stationary or have velocities up to 50 km/h. The UDN-ANs' power budget is varied from 0dBm to 30dBm. Results show that near-equal division between backhaul and access network throughput is achieved when the power budget for the UDN-ANs is 20dBm. These results also show that the proposed in-band scheme reaches ∼58% of the performance achievable with ideal backhaul while only ∼24% of M-MIMO backhaul performance is lost due to interference caused by UDN-ANs (red line).

mechanically according to the METIS guidelines for simulating a similar Madrid grid based dense urban information society scenario [20]. Constant 49dBm power budget was used on each M-MIMO-AN. The UDN-ANs consisted of two antenna arrays: one for the access network and another for the backhaul. The antenna array for the backhaul was a linear array of 2 dual-polarized dipoles while the antenna array for the access network consisted of 20 dual-polarized 3GPP patch antennas on a circular geometry. The multiantenna transceivers at the UDN-ANs for the access network and backhaul were placed at 5 m and 6m height above the ground, respectively.

The antenna arrays employed by the UNs consisted of linear arrays with 2 dual-polarized dipoles at a height of around 1.5m above the ground. A user density of 1000 users/km^2 was used. Users were randomly dropped on the streets of the Madrid grid and their velocities ranged from 0km/h to 50km/h. We have assumed that the data traffic is dominated by DL, hence the allocation between physical resources was 83 % for DL and 17 % for UL. CSI estimation with pilot contamination was taken into account in simulations similarly as in [5]. In order to avoid significant pilot contamination and inter-symbol interference CSI beacon allocations were planned spatially as described in [21]. Resource allocation between the backhaul and the access network was done in terms of transmission power domain for DL and in TDD for UL. Two spatial backhaul streams were assumed for each UDN-AN. Further parameters employed in the simulation are given in Table 2.

A. DOWNLINK PERFORMANCE

Fig. 4 illustrates the overall performance of proposed C-UDN system, with and without in-band backhauling, in terms of mean AN throughput. It can be observed that when power budget for the UDN-ANs increases the backhaul reception deteriorates due to increased interference. When the power budget for each M-MIMO-AN is 49dBm, as assumed in this study, then 20dBm power budget for the UDN-ANs gives near-equal division between backhaul and access network throughput.

Results also show that an improvement in terms of throughput is achieved when users measure DL precoded reference signals, transmitted by the M-MIMO-ANs during measurement gaps, in order to mitigate in-band backhaul interference (green bars in Fig. 4). Note that a measurement gap periodicity of 5 ms was assumed. When users are moving at 50km/h, the ability of users in cancelling backhaul interference decreases slightly compared with a fully stationary scenario.

The proposed in-band scheme reaches ∼58% of the UDN performance achievable with ideal (e.g., high-capacity wired) backhaul. Moreover, only ∼24% of M-MIMO backhaul performance is lost due to interference caused by UDN-ANs compared to the (ideal) case where the proposed wireless backhaul solution is not subject to interference from the UDN (red line in Fig. 4).

These results show that the proposed in-band backhauling scheme yields larger throughput compared to a TDD solution for in-band wireless backhaul of UDNs in DL. For example, a resource allocation of 58 % for backhaul and 42% for the access network yields an average throughput of 421 Mbps and 422 Mbps, respectively. Hence, an ∼30% increase in throughput can be achieved with the proposed in-band backhauling solution compared to such a TDD scheme.

Furthermore, comparing the results in Fig. 4 for mobile users (50km/h) to those in [5] shows that serving users with C-UDNs and using M-MIMO for in-band backhaul is a much more efficient solution (in terms of throughput)

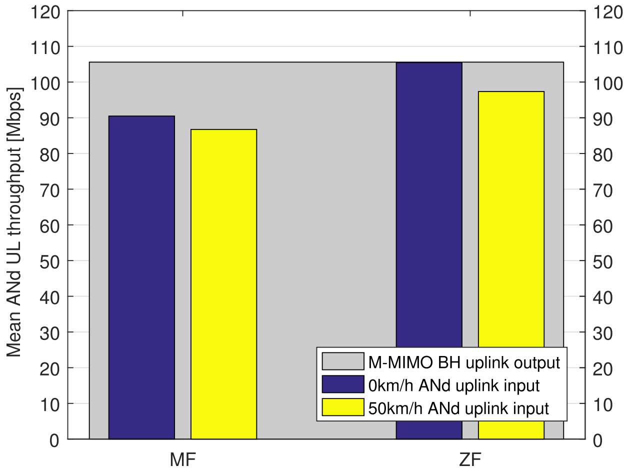

FIGURE 5. Performance of the proposed in-band backhaul scheme in terms of average UL throughput per UDN-AN. Results show that the average throughput that is available per UDN-AN for backhaul is only slightly larger than that required for handling (or forwarding) the access network transmissions when 35% of subframes are allocated for backhaul and the remaining 65% for UL access. Hence, a 35/65 resource allocation scheme provides a good trade-off of radio resources available for backhaul and access network for the proposed in-band solution.

compared to the case where vehicular users are served directly by M-MIMO systems deployed on a macro-cell setting.

B. UPLINK PERFORMANCE

Figure 5 illustrates the performance of the proposed in-band backhaul scheme in terms of average UL throughput. We have considered that 35 % of subframes are allocated for backhaul and the remaining 65 % for UL access. Results show that the average throughput that is available per UDN-AN for backhaul is only slightly larger than that required for handling (or forwarding) the access network transmissions. Hence, a 35/65 resource allocation scheme provides a good trade-off of radio resources available for backhaul and access network.

VII. CONCLUSIONS AND FUTURE WORK

We have shown that in-band backhaul for 5G ultra-dense networks using massive MIMO systems is a feasible and cost-efficient alternative to using mmW or wired based solutions. In particular, we have proposed a scheme where in-band simultaneous downlink transmissions in the backhaul and access network are made possible by exploiting state-of-the-art practical MU-MIMO techniques and multiantenna tranceivers. A novel frame structure has also been proposed for allowing a co-existence between in-band massive MIMO based backhaul and ultra-dense networks.

Naturally, the best overall performance in terms of throughput is obtained using a backhaul technology that is either based on high-capacity mmW or wired connections. In particular, the proposed scheme reaches ∼58% of the access network performance achievable with ideal (e.g., wired) backhaul. However, in practice it may be very challenging to provide backhaul for all access nodes composing the ultra-dense network in a cost-efficient manner either with mmW or high-capacity wired based technologies due to typical line-of-sight requirements and required infrastructure. The solution proposed in this paper has the advantages of reusing both the spectrum in sub-6 GHz and macro-sites as well as providing a smooth transition from LTE to 5G networks. Finally, our numerical results have shown that the proposed solution for in-band backhauling of UDNs provides an ∼30% increase in throughput compared to a TDD scheme.

ACKNOWLEDGMENT

The authors would like to thank Panu Johansson, senior user interface concept designer at Huawei Technologies Oy (Finland) Co. Ltd., for his concept art work used for illustrating C-UDN and M-MIMO interoperation.

REFERENCES

[1] Huawei Technologies Co, *5G: New Air Interface and Radio Access Virtualization*. (2015). [Online]. Available: http://www.huawei.com/minisite/has2015/img/5g_radio_whitepaper.pdf
[2] NGMN Alliance. (2015). *NGMN 5G White Paper*. [Online]. Available: https://www.ngmn.org/uploads/media/NGMN_5G_White_Paper_V1_0.pdf
[3] *Study on Scenarios and Requirements for Next Generation Access Technologies in V14.0.0*, document. 3GPP TS 38.913, Oct. 2016.
[4] N. Bhushan *et al.*, "Network densification: The dominant theme for wireless evolution into 5G," *IEEE Commun. Mag.*, vol. 52, no. 2, pp. 82–89, Feb. 2014.
[5] P. Kela *et al.*, "Supporting mobility in 5G: A comparison between massive MIMO and continuous ultra dense networks," in *Proc. IEEE Int. Conf. Commun. (ICC)*, May 2016, pp. 1–6.
[6] E. G. Larsson, O. Edfors, F. Tufvesson, and T. L. Marzetta, "Massive MIMO for next generation wireless systems," *IEEE Commun. Mag.*, vol. 52, no. 2, pp. 186–195, Feb. 2014.
[7] N. Alliance. (Jun. 4, 2012). *NGMN Small Cell Backhaul Requirements White Paper*. [Online]. Available: https://www.ngmn.org/uploads/media/NGMN_Whitepaper_Small_Cell_Backhaul_Requirements.pdf
[8] S. Hur, T. Kim, D. J. Love, J. V. Krogmeier, T. A. Thomas, and A. Ghosh, "Millimeter wave beamforming for wireless backhaul and access in small cell networks," *IEEE Trans. Commun.*, vol. 61, no. 10, pp. 4391–4403, Oct. 2013.
[9] Z. Pi, J. Choi, and R. W. Heath Jr, "Millimeter-wave Gbps broadband evolution towards 5G: Fixed access and backhaul," *IEEE Commun. Mag.*, vol. 54, no. 4, pp. 138–144, Apr. 2016.
[10] World Radiocommunication Conference, *Final Acts WRC-15*. (2015). [Online]. Available: http://www.itu.int/pub/R-ACT-WRC.12-2015/en
[11] B. Li, D. Zhu, and P. Liang, "Small cell in-band wireless backhaul in massive MIMO systems: A cooperation of next-generation techniques," *IEEE Trans. Wireless Commun.*, vol. 14, no. 12, pp. 7057–7069, Dec. 2015.
[12] H. Tabassum, A. H. Sakr, and E. Hossain, "Analysis of massive MIMO-enabled downlink wireless backhauling for full-duplex small cells," *IEEE Trans. Commun.*, vol. 64, no. 6, pp. 2354–2369, Jun. 2016.
[13] R.-A. Pitaval, O. Tirkkonen, R. Wichman, K. Pajukoski, E. Lahetkangas, and E. Tiirola, "Full-duplex self-backhauling for small-cell 5G networks," *IEEE Wireless Commun. Mag.*, vol. 22, no. 5, pp. 83–89, Oct. 2015.
[14] P. Kela *et al.*, "Location based beamforming in 5G ultra-dense networks," in *Proc. IEEE 84th Veh. Technol. Conf. (VTC2016-Fall)*, Sep. 2016.
[15] J. Werner, M. Costa, A. Hakkarainen, K. Leppanen, and M. Valkama, "Joint user node positioning and clock offset estimation in 5G ultra-dense networks," in *Proc. IEEE Global Commun. Conf. (GLOBECOM)*, Dec. 2015, pp. 1–7.
[16] H. Q. Ngo, E. Larsson, and T. Marzetta, "Massive MU-MIMO downlink TDD systems with linear precoding and downlink pilots," in *Proc. 51st Annu. Allerton Conf. Commun. Control, Comput. (Allerton)*, Oct. 2013, pp. 293–298.
[17] Q. H. Spencer, A. L. Swindlehurst, and M. Haardt, "Zero-forcing methods for downlink spatial multiplexing in multiuser MIMO channels," *IEEE Trans. Signal Process.*, vol. 52, no. 2, pp. 461–471, Feb. 2004.

[18] METIS, *METIS Channel Models*. (2015). [Online]. Available: https://www.metis2020.com
[19] *Study on 3D Channel Model for LTE (Release 12)*, document. 3GPP TR 36.873, Jun. 2015. [Online]. Available: http://www.3gpp.org
[20] METIS, *Scenarios, Requirements and KPIs for 5G Mobile and Wireless System*. (2013). [Online]. Available: https://www.metis2020.com
[21] P. Kela, J. Turkka, and M. Costa, "Borderless mobility in 5G outdoor ultra-dense networks," *IEEE Access*, vol. 3, pp. 1462–1476, Aug. 2015.
[22] METIS, *Scenarios, Requirements and KPIs for 5G Mobile and Wireless System*. (2013). [Online]. Available: https://www.metis2020.com

PETTERI KELA (M'15) received the M.Sc. degree from the University of Jyväskylä, Finland, in 2007. From 2001 to 2007, he was with the Department of Mathematical Information Technology, University of Jyväskylä. He joined Nokia, as a Protocol Design Engineer, where he has been involved in LTE UE modem software development. From 2010 to 2013, he was a Senior Researcher and a Technical Lead with Renesas Mobile Corporation, where he was involved in LTE-A system research, and L1/L2 modem software architecture and implementation. Since 2013, he has been with Huawei Technologies Oy (Finland) Company, Ltd., as a Senior Researcher. He is also part-time doctoral student with the School of Electrical Engineering, Aalto University. His research interests include 5G, L1/L2 protocols, ultra-dense networks, and multi-user MIMO techniques.

MÁRIO COSTA (S'08–M'13) was born in Portugal in 1984. He received the M.Sc degree (Hons.) in communications engineering from the Universidade do Minho, Portugal, in 2008, and the D.Sc. (Tech.) degree in electrical engineering from Aalto University, Finland, in 2013. From 2007 to 2014, he was with the Department of Signal Processing and Acoustics, Aalto University. In 2011, he was an External Researcher with the Connectivity Solutions Team, Nokia Research Center. He was a Visiting Post-Doctoral Research Associate with Princeton University in 2014. Since 2014, he has been with Huawei Technologies Oy (Finland) Company, Ltd., as a Senior Researcher. His research interests include statistical signal processing and wireless communications.

JUSSI TURKKA (S'08–M'14) received the M.Sc. and D.Sc. (Tech) degrees from the Tampere University of Technology, Finland, in 2008 and 2014, respectively. He has been with Magister Solutions Ltd., since 2009, as a Senior Research Consultant for several projects. Since 2016, he has been with the European Communications Engineering Ltd. He has been authoring several scientific publications and contributing to 3GPP specifications. His areas of expertise are in the field of self-organizing cellular networks, mobility robustness optimization, minimization of drive tests and knowledge mining.

KARI LEPPÄNEN received the M.Sc. and Ph.D. degrees from the Helsinki University of Technology, Finland, in 1992 and 1995, respectively, major in space technology and radio engineering. He was with the National Radio Astronomy Observatory, USA, the Helsinki University of Technology, Finland, the Joint Institute for VLBI in Europe, The Netherlands, and the Nokia Research Center, Finland. He currently leads the 5G Radio Network Technologies Team at Huawei in Stockholm and Helsinki.

RIKU JÄNTTI (M'02–SM'07) received the M.Sc. degree (Hons.) in electrical engineering and the D.Sc. degree (Hons.) in automation and systems technology from the Helsinki University of Technology in 1997 and 2001, respectively. He was a Professor pro tem with the Department of Computer Science, University of Vaasa. He is currently an Associate Professor in communications engineering and the Head with the Department of Communications and Networking, School of Electrical Engineering, Aalto University, Finland. He is an Associate Editor of the IEEE Transactions on Vehicular Technology. He is also the IEEE VTS Distinguished Lecturer (Class 2016). His research interests include radio resource control and optimization for machine type communications, cloud based radio access networks, spectrum and co-existence management and RF Inference.